The American Journal of Pathology, Vol. 174, No. 5, May 2009

DOI: 10.2353/ajpath.2009.080890

Epithelial and Mesenchymal Cell Biology

The Transmembrane src Substrate Trask Is an Epithelial Protein that Signals during Anchorage Deprivation

Danislav S. Spassov,* Frederick L. Baehner,† Ching Hang Wong,* Stephen McDonough,* and Mark M. Moasser*

From the Departments of Medicine, and Pathology,† University of California, San Francisco, San Francisco, California*

The roles of epithelial cells encompass both cellular- and tissue-level functions that involve numerous cell–cell and cell–matrix interactions, which ultimately mediate the highly structured arrangement of cells on a basement membrane. Although maintaining this basic structure is critical for preserving tissue integrity, plasticity in epithelial cell behavior is also critical for processes such as cell migration during development or wound repair, mitotic cell detachment, and physiological shedding. The mechanisms that mediate epithelial cell plasticity are only beginning to be understood. We previously identified Trask, a transmembrane protein that is phosphorylated by src kinases during mitosis. In this study, we report that the phosphorylation of Trask is associated with anchorage loss in epithelial cells. Phosphorylation of Trask is seen during the cell-detachment phase of mitosis, in experimentally induced interphase detachment, and during cell migration in experimental epithelial models. An analysis of human tissues shows that Trask is widely expressed in many epithelial tissues but not in most tissues of mesenchymal origin, except for a subset of early hematopoietic cells. Trask is not phosphorylated in epithelial tissues *in vivo*; however, its phosphorylation is seen in epithelial cells undergoing mitosis or physiological shedding. Trask is a novel epithelial membrane protein that is phosphorylated by src kinases when epithelial cells disengage from their tissue framework, identifying an important new regulator of epithelial tissue dynamics. ***(Am J Pathol 2009, 174:1756–1765; DOI: 10.2353/ajpath.2009.080890)***

A hallmark of epithelial tissue architecture is the highly ordered arrangement of cells on a basement membrane. The cellular engagement to substratum administers structural attributes to the tissue, but also specifies cellular functions including shape, polarity, and survival. During processes such as mitosis or cell migration, epithelial cells must sever cell–matrix and cell–cell engagements to execute migratory or mitotic functions. Separation from basement membrane requires activation of signaling pathways unique to the anchorage-independent state, not only to compensate for the loss of anchorage-driven signals such as survival, but also to execute specific cellular attributes such as shape, membrane, and cytoskeletal structure, and the ability to seek and restore anchorage and reconstruct the epithelial architecture. Some of the changes associated with the migration of epithelial cells have been described as epithelial mesenchymal transition. The epithelial mesenchymal transition, as described, is a process that is mediated through gene transcription and involves loss of expression of certain proteins characteristic of epithelial cells and induction of expression of certain proteins characteristic of mesenchymal cells.[1] However, processes such as mitotic epithelial cell detachment and rounding depend on more rapid signaling mechanisms, such as those mediated through tyrosine phosphorylation of membrane proteins. The mechanisms that regulate the structural and functional changes during epithelial cell mitosis are not yet known.

The src family of non-receptor tyrosine kinases are multifunctional proteins involved in diverse cellular processes that include regulation of the actin cytoskeleton,

Supported by the National Institutes of Health grant CA113952 and the American Cancer Society RSG-0213901CDD. D.S. is supported by a Susan G. Komen for the Cure postdoctoral fellowship. C.H.W. is supported by a California Breast Cancer Research Program Post-doctoral fellowship.

D.S.S. and F.L.B. contributed equally to this work.

Accepted for publication February 3, 2009.

Supplemental material for this article can be found on *http://ajp.amjpathol.org.*

Address reprint requests to Mark M. Moasser, Associate Professor, University of California, San Francisco, UCSF Box 0875, San Francisco, CA 94143-0875. E-mail: mark.moasser@ucsf.edu.

and cell–cell and cell–substratum interactions. Among other functions, src kinases have long been presumed to have a mitotic function.[2,3] This presumption has been born out of experiments that show increased activity of src during mitosis,[4,5] mitotic phosphorylation of src by cdc2,[6] relocalization of src during mitosis,[7] and conformational changes that are consistent with mitosis-specific substrate recognition.[8] However the mitotic function of src has remained elusive, and a reasonable hypothesis regarding this function has been awaiting the identification of a functionally revealing substrate for src during mitosis. Looking for mitotic substrates of src kinases, we recently described the cloning and identification of a novel mitotic substrate of src kinases named Trask.[9] Trask is expressed as a full length 140-kDa and a cleaved 85-kDa transmembrane glycoprotein and other than the presence of extracellular complement C1r/Cls, Uegf, Bmp1 domains shows little homology to known protein families. Trask interacts with the membrane protease MT-SP1 and the 140-kDa Trask protein is proteolytically cleaved by MT-SP1 within the extracellular domain to generate the 85-kDa form of Trask. The functional relevance of this cleavage is not yet known. Trask is only seen in more complex metazoans and undergoes src family kinase dependent tyrosine phosphorylation during mitosis. Trask was also independently identified in microarray studies as a transcript overexpressed in colon cancers and named CDCP1[10] and in subtractive immunization studies as a surface antigen with increased expression in a highly metastatic variant of HEp3 carcinoma cells and named SIMA135.[11] Since Trask has little homology to other proteins, predictive approaches do not shed light on its cellular functions. We previously showed that the forced overexpression and overphosphorylation of Trask interferes with cell spreading without interfering with cell proliferation.[9] We have now studied the mitotic phosphorylation of Trask in more depth and report that Trask phosphorylation coincides with mitotic cell detachment and not with the mitotic cell cycle. Trask remains phosphorylated in the post mitotic G1 phase until cells reattach to matrix. Trask phosphorylation is also seen when interphase epithelial cells are experimentally forced to detach, and can be seen in detached mitotic or interphase epithelial cells *in vivo* or in cells preparing for physiological shedding.

Materials and Methods

Cell Culture and Reagents

All cell lines were obtained from the American Type Culture Collection. Cells were grown in a 1:1 mixture of Dulbecco's Modified Eagle Medium:F12 media supplemented with 10% heat-inactivated fetal bovine serum, and 100 U/ml penicillin, 100 μg/ml streptomycin, 4 mmol/L glutamine, and incubated at 37 C in 5%CO2. MCF10A cells were grow in Dulbecco's Modified Eagle Medium:F12 media supplemented with 5% donor horse serum, 0.5 μg/ml hydrocortisone, 10 μg/ml insulin, 20 ng/ml epidermal growth factor, 100 U/ml penicillin, 100 μg/ml streptomycin, and 4 nmol/L glutamine. To force cells into suspension, cells were washed in PBS and exposed to a 0.05% solution of trypsin or a 2 mmol/L solution of EDTA in Hanks' buffer. When required to maintain cells in suspension and prevent spreading and attachment, cells were spun down, resuspended in growth media, and cultured in ULC plates (Corning) for growth. To harvest lysates, cells were rapidly scraped on ice at fixed time points and lysed in RIPA buffer. For wound healing experiments, near-confluent MCF10A cells growing on round coverslips were mechanically scraped across the equator to generate a cell-free zone, placed back into the incubator, and examined under the microscope periodically. When cells were found to be migrating into the gap, they were fixed and stained as indicated. Anti-phosphotyrosine antibodies (PY99) were purchased from SantaCruz Biotechnology, Inc (SantaCruz, CA). Polyclonal anti-Trask antibodies were generated by immunizing rabbits with a recombinant full-length Trask intracellular domain. Monoclonal anti-Trask antibodies were generated by immunizing mice with a recombinant full-length Trask extracellular domain and recognize both cleaved and uncleaved forms of Trask. Anti-phospho-Trask antibodies were generated against a phospho-peptide immunogen containing sequences centered around phosphorylated tyrosine 743 of Trask in rabbits and affinity purified on a phospho-peptide column. Conditions for immunohistochemical staining of paraffin embedded tissues were established and the specificity of these immunostains for Trask and phospho-Trask were confirmed using formalin-fixed paraffin embedded positive and negative controls from cell lines that express or do not express Trask, and from cell lines with constitutively phosphorylated Trask or dephosphorylated Trask due to Src inhibitor pretreatment (supplementary Figure S1 at *http://ajp.amjpathol.org*). For knockdown experiments MCF10A cells were seeded in 6-well clusters and transfected with anti-Trask small interfering (si)RNA or non-targeting control siRNA pools (Dharmacon siGenome SMARTpool #M-010732-00 and D-001206-14) at 100 nmol/L using Lipofectamine 2000 according to the manufacturer's protocol.

Fluorescence-Activated Cell Sorting Analysis

For analysis of DNA content, cell nuclei were prepared as previously described (Moasser et al, 1999) and DNA content was determined by flow cytometric analysis of red fluorescence of the 488 nm excited ethidium bromide stained nuclei.

Immunoblotting and Immunofluorescent Studies

Total cellular lysates were harvested in modified RIPA buffer (10 mmol/L Na phosphate [pH 7.2], 150 mmol/L NaCl, 0.1% SDS, 1% NP40, 1% Na deoxycholate, protease inhibitors and 1 mmol/L sodium orthovanadate). For Western blotting, 50 μg of each lysate was separated by SDS-polyacrylamide gel electrophoresis, transferred to membrane, and immunoblotted using appropriate

primary and secondary antibodies and enhanced chemoluminescence visualization. For immunolocalization studies, cells were grown on fibronectin-coated glass coverslips and fixed with 4% paraformaldehyde and permeabilized with triton ×-100. Fixed cells were incubated with primary antibody and subsequently with rhodamine Red or Alexa 488 conjugated secondary antibodies (Molecular Probes) and visualized under fluorescent microscopy. Actin staining was done using phalloidin-fluorescein isothiocyanate conjugate.

Immunohistochemical Studies

Deparaffinized sections were rehydrated and antigen retrieval performed by 15 minutes incubation in warm trypsin followed by microwaving in 10 mmol/L citrate buffer for total of 10 minutes in 1-minute intervals. Slides were then washed and blocked with 3% H_2O_2 followed by blocking in goat serum and primary incubation at 4°C overnight. Secondary staining was performed using biotinylated goat anti-rabbit antibodies (Vector Labs, Burlingame, CA) and colorized using Vectastain ABC Kit (Vector Labs) and 3,3′-diaminobenzidine- H_2O_2 substrate (Sigma, St, Louis, MO). Slides were then counterstained with hematoxylin, dehydrated through graded alcohols and xylene and mounted. Slides were studied and imaged under brightfield microscopy. All staining procedures included positive and negative controls. Controls were prepared from formalin-fixed paraffin embedded cell buttons of cell lines with well-defined expression and phosphorylation of Trask by immunoblotting techniques. For Trask immunostains the positive control was MDA-MB-468 cells and the negative control was MCF-7 cells. For phospho-Trask immunostains the positive control was MDA-MB-468 cells and the negative controls were MCF-7 cells and dasatinib-treated MDA-MB-468 cells. Staining intensity was scored and agreed on by two investigators according to the following definitions: 0 indicates no visible expression (similar to negative controls); 1+ indicates expression that is faint but is identifiable and above background and negative controls; 2+ indicates moderate expression that is clearly evident but also clearly less intense than positive controls; and 3+ indicates intense expression similar to positive controls. Only intensity was used for scoring. Percentages of cells was not a parameter used for scoring since Trask phosphorylation has focal characteristics in tissues that is relevant to cell behavior, and some degree of focal variability may also be due to uneven fixation artifacts.

Microscopy

Tissue cultured cells were viewed and imaged by phase contrast microscopy using a Nikon TS-100F inverted microscope equipped with a Nikon D100 digital camera attached to the photo port. Images were imported into Photoshop software, converted to gray scale, and gamma-adjusted for optimal representation. Fluorophore stained cells were imaged by fluorescence microscopy using an Axioplan 2 Zeiss microscope at the appropriate excitation wavelengths. Zeiss Fluar objective lenses were used with immersol 518N as imaging medium. Pictures were taken at room temperature with Axiocam MRm camera and Axiovision 4.5 acquisition software, imported into Photoshop software and gamma adjusted for optimal representation. Immunohistochemically stained tissue sections were viewed and imaged using an Olympus BX41 brightfield microscope fitted with a DP70 digital camera. Images were acquired using the Olympus DP Controller software and gamma adjusted for optimal representation.

Results

We previously showed that MDA-468 cells undergo Trask phosphorylation during the mitotic phase.[9] In the current study, we examined the mitotic phosphorylation of Trask more closely. Mitotic MDA-468 cells were collected by shake-off after 20 hours of nocodazole treatment, washed, and replated onto tissue culture plates. At sequential time points, the cell cycle phase and the expression and phosphorylation of Trask were determined in these cells. Mitotic MDA-468 cells are entirely round and suspended at collection and at the initial time of replating (Figure 1A, 1B, time 0). After release from mitotic block, they slowly resume cell cycle progression and proceed to complete the mitotic phase. Entry into G1 phase begins sometime after 0.5 hours and is complete by 2 hours after nocodazole release (Figure 1A). However, the rounded shape persists within the initial 1 to 2 hours of G1 such that the majority of cells at the 2 to 3-hour time point are G1 cells that are round, but have not yet spread onto plastic (Figure 1A, 1B, 2 to 3-hour time points, and Figure 1C) (see supplementary Figure S2 at *http://ajp.amjpathol.org* for the full collection of images). When the phosphorylation of Trask is examined at each of these time points, it is apparent that Trask phosphorylation is not linked with the mitotic phase; rather it is linked with cell spreading. Trask continues in the phosphorylated state when cells are in G1 (Figure 1A, 1D, 2 to 3-hour time points) and becomes dephosphorylated when cells spread and reattach (Figure 1B, 1D, 4 to 6-hour time points). Therefore Trask phosphorylation is linked with the cell detachment and respreading that occurs in mitotic epithelial cells, not the cell cycle checkpoints of mitosis.

In fact examination of spontaneous mitoses in asynchronous cell populations without the use of nocodazole shows that not all mitoses have phosphorylation of Trask. Some cells in early prophase, before cell detachment, show no phosphorylation of Trask, whereas cells in later stages of mitosis show phosphorylation of Trask (Figure 2A). If Trask is maintained in the hyperphosphorylated state through overexpression, cells undergo mitotic cell detachment normally, but are deficient in respreading after completion of mitosis and continue proliferative activity in the suspended state, leading to gradual accumulation of suspended cells with repeated cell divisions (supplementary Movies M1, M2 at *http://ajp.amjpathol.org*). These data suggested that phosphorylation of Trask is linked with the detached or suspended state of epithe-

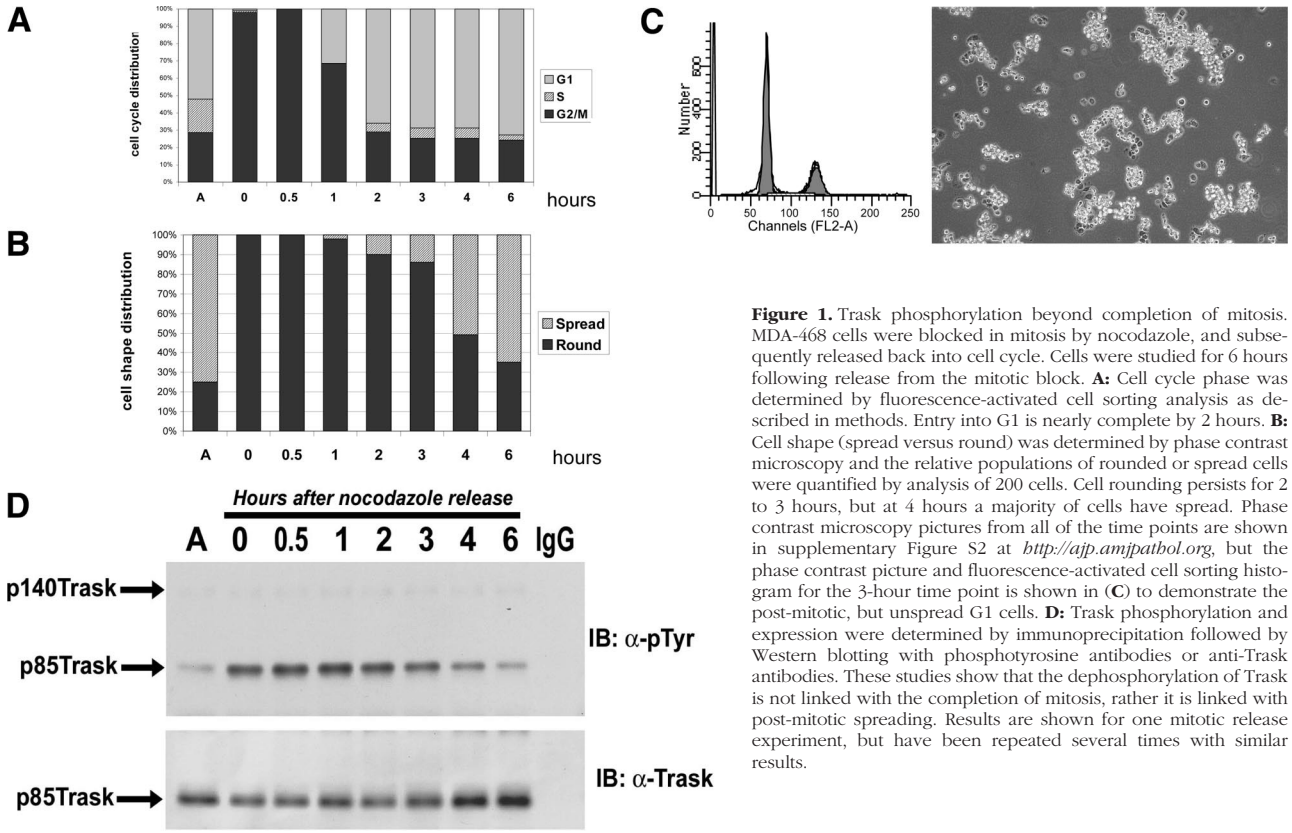

Figure 1. Trask phosphorylation beyond completion of mitosis. MDA-468 cells were blocked in mitosis by nocodazole, and subsequently released back into cell cycle. Cells were studied for 6 hours following release from the mitotic block. **A:** Cell cycle phase was determined by fluorescence-activated cell sorting analysis as described in methods. Entry into G1 is nearly complete by 2 hours. **B:** Cell shape (spread versus round) was determined by phase contrast microscopy and the relative populations of rounded or spread cells were quantified by analysis of 200 cells. Cell rounding persists for 2 to 3 hours, but at 4 hours a majority of cells have spread. Phase contrast microscopy pictures from all of the time points are shown in supplementary Figure S2 at *http://ajp.amjpathol.org*, but the phase contrast picture and fluorescence-activated cell sorting histogram for the 3-hour time point is shown in (**C**) to demonstrate the post-mitotic, but unspread G1 cells. **D:** Trask phosphorylation and expression were determined by immunoprecipitation followed by Western blotting with phosphotyrosine antibodies or anti-Trask antibodies. These studies show that the dephosphorylation of Trask is not linked with the completion of mitosis, rather it is linked with post-mitotic spreading. Results are shown for one mitotic release experiment, but have been repeated several times with similar results.

lial cells, leading us to look for more evidence of Trask phosphorylation in non-mitotic cells.

MDA-468 cells have some phosphorylation of Trask even during interphase. Interestingly, these cells grow with a semiadherent morphology in cell culture such that many of the cells spread and flatten and many of them remain in a loosely attached rounded morphology. Staining these cells with anti-p-Trask antibodies shows that the rounded subpopulation of cells have intense Trask phosphorylation whereas the flattened cells have much less (Figure 2B). These are not mitotic cells as evidenced by 4,6-diamidino-2-phenylindole staining of nuclear chromatin. MCF10A cells, on the other hand, are flattened epithelial cells that grow in fully adherent morphology. When these cells are stained with anti-p-Trask antibodies, there is little, if any, phosphorylation of Trask in the majority of cells, which are spread and in interphase. However occasional detached mitotic cells show intense phosphorylation of Trask (Figure 2, C and D). Comparing the semi-adherent MDA-468 epithelial cells with fully spread MCF10A epithelial cells and epithelial cells that naturally grow in a completely suspended morphology (DU-4475) further confirms that Trask phosphorylation is linked with cell attachment. Asynchronous MCF10A cells, which grow in flattened monolayer, have little phosphorylation of Trask during interphase, but induce Trask phosphorylation during mitotic detachment (Figure 2E). MDA-468 cells, which grow in semisuspended morphology, have modest Trask phosphorylation representing a mixture of cell morphologies, which becomes maximal during mitotic detachment (Figure 2E). In contrast, DU-4475 cells, which do not adhere to plastic and naturally grow in a fully suspended morphology, have maximal phosphorylation of Trask during interphase with no further increase during mitosis (Figure 2E). This further confirms that the phosphorylation of Trask is linked with the suspended and detached state of epithelial cells.

To further study the relationship between Trask and the state of adhesion, we studied MCF10A immortalized epithelial cells, which grow in an entirely flattened typical epithelial cell morphology, have abundant expression of Trask, and barely detectable phosphorylation of Trask during interphase. MCF10A cells were forced to detach from matrix by treatment with 2 mmol/L EDTA. Analysis of Trask phosphorylation by immunoprecipitation and anti-phosphotyrosine immunoblotting shows that Trask is tyrosine phosphorylated as these cells detach from substrate (Figure 3A). Similar results are seen when primary keratinoctyes are forced to detach by exposure to EDTA (data not shown).

The detachment experiments were repeated to determine the onset, duration, and endpoint of Trask phosphorylation. These cells were exposed to a solution containing trypsin, and rapidly lysed at several time points corresponding to the onset of cell rounding, the onset of cell detachment, and full suspension for short and long periods. Trypsinized cells were then replated in regular media and rapidly lysed at time points corresponding to before and after re-spreading. Trypsin rapidly cleaves Trask to its 85-kDa form (Figure 3B, lower panel, compare lanes 1 & 2). The cleavage of Trask by serine proteases and the exact site of cleavage was previously de-

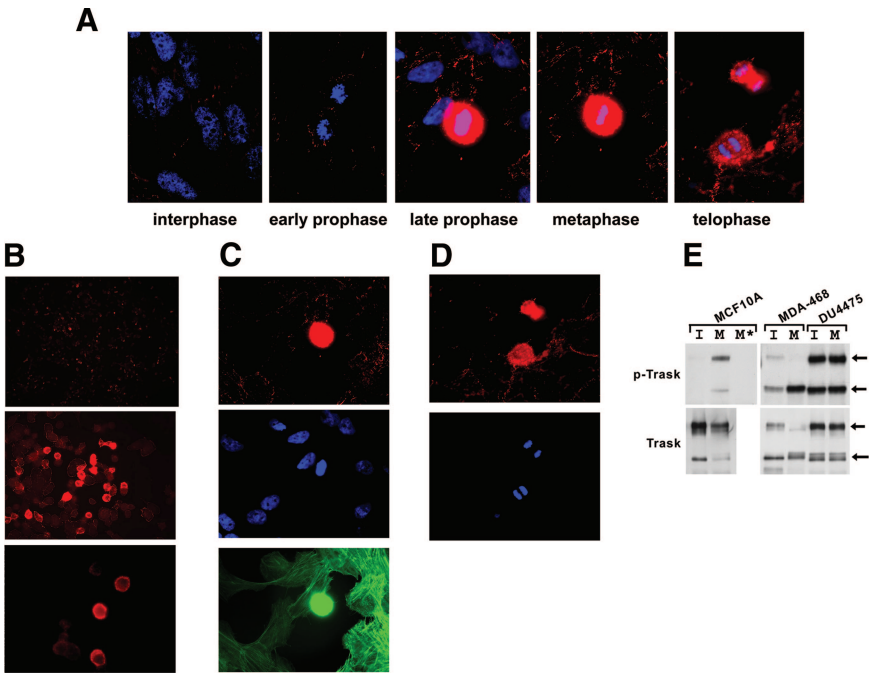

Figure 2. Trask phosphorylation in non-manipulated cells. **A:** MDA-468 cells were grown on fibronectin-treated coverslips and were fixed in log phase without any drug treatment or experimental interventions and stained with anti-p-Trask antibodies, rhodamine-conjugated secondary antibodies, and 4,6-diamidino-2-phenylindole. Most cells have only sparse phosphorylation of Trask. Mitotic cells were identified on the coverslip by their characteristic chromatin condensation pattern and numerous mitotic cells in different phases of mitoses were imaged. Intense Trask phosphorylation is seen in detached mitotic cells. (×1000 magnification) **B:** In addition, many rounded interphase cells also have Trask phosphorylation. Rounded cells are commonly seen in cultures of MDA-468 cells, which typically grow in a semisuspended morphology with many spread and many loosely attached rounded cells. (×50, ×400, ×400 magnification) **C,D:** MCF10A cells were similarly grown on coverslips, fixed, and stained with anti-p-Trask antibodies (red), 4,6-diamidino-2-phenylindole (blue), and fluorescein isothiocyanate-conjugated phalloidin (green) to visualize the actin cytoskeleton. Spontaneous mitotic cells were located and identified by their chromatin condensation and cell rounding. (**C**) shows a rounded cell in later prophase among many flattened interphase cells. (**D**) shows two anaphase cells (×1000 magnification). **E:** Interphase (labeled I) and nocodazole-blocked mitotic (labeled M) cultures of MCF10A, MDA-468, and DU4475 cells were harvested and Trask expression and phosphorylation determined by anti-Trask immunoprecipitation and anti-ptyr immunoblotting. **Arrows** indicate the p140 and p85 forms of Trask. The M* lane was immunoprecipitated with an IgG control antibody.

scribed.[9] Phosphorylation of Trask is induced at the very onset of cell rounding, before detachment (Figure 3B, lane 2), and peaks when cells are completely detached and suspended (Figure 3B, lane 4). After inactivation of trypsin and incubation in media, Trask phosphorylation is maintained for prolonged periods as long as cells are kept in suspension (Figure 3B, lanes 5 and 6). With prolonged culture in suspension, newly synthesized uncleaved 140-kDa Trask eventually predominates and is also phosphorylated (Figure 3B, lane 6). When cells are replated onto tissue culture treated plates, phosphorylation of Trask is maintained during the first hour when cells are loosely adhered but still round (Figure 3B, lane 7). However, with spreading and flattening of these cells during the second hour, Trask is dephosphorylated (Figure 3B, lanes 8 and 9). The detachment of cells from plastic in sheets (by mechanical scraping) does not lead to Trask phosphorylation (Figure 3B, lane 10). This is likely due to the fact that cell scraping removes intact cell clusters and their underlying matrix proteins en-block, maintaining much of the cell-matrix and cell-cell interactions, unlike EDTA or trypsin, which sever cell-matrix and cell-cell interactions, resulting in cell retraction and rounding. Therefore the phosphorylation of Trask is tightly linked with cell retraction from matrix and ends when anchorage to substratum is re-established. If Trask phosphorylation is forcibly maintained by overexpression, trypsinized cells will not respread on substratum as previously shown using engineered MDA-468 cells.[9]

The phosphorylation of Trask with detachment-induced cell retraction is seen in a punctate membrane and cytoplasmic pattern and significantly intensifies in suspension (Figure 4A). If Trask phosphorylation is suppressed by treatment with a src selective tyrosine kinase inhibitor, cell retraction and rounding induced by trypsin is severely impaired, and cells are unable to release cell-cell contacts, and filamentous actin supported protrusions keep cells in touch with each other despite cytoplasmic retraction (Figure 4B). This phenotype induced by src inhibitor treatment may be in part related to numerous other cellular substrates, in addition to Trask, that are dephosphorylated on src inhibitor treatment. Therefore to more specifically study the role of Trask in detachment-induced cell retraction we studied the effect of Trask siRNA knockdown on detachment (Figure 4C). Cells lacking Trask expression due to siRNA knockdown are similarly significantly impaired in their ability to retract and enter into suspension and are similarly unable to disassemble filamentous protrusions, while control siRNA treated cells rapidly retract, round, and assume a suspended morphology (Figure 4D). Taken together, the src inhibitor and siRNA data confirm that the phosphorylation of Trask is an important mediator of cell retraction and rounding in response to the loss of anchorage.

The Trask overexpression studies, and the src inhibitor and Trask siRNA experiments all seem to be consistent with a Trask function in regulating the actin dynamics. Another circumstance wherein epithelial cells require remodeling of the actin cytoskeleton is during cell migration. Therefore we looked for evidence of Trask phosphorylation during epithelial cell migration. To study this, we induced cell migration by introducing a linear wound

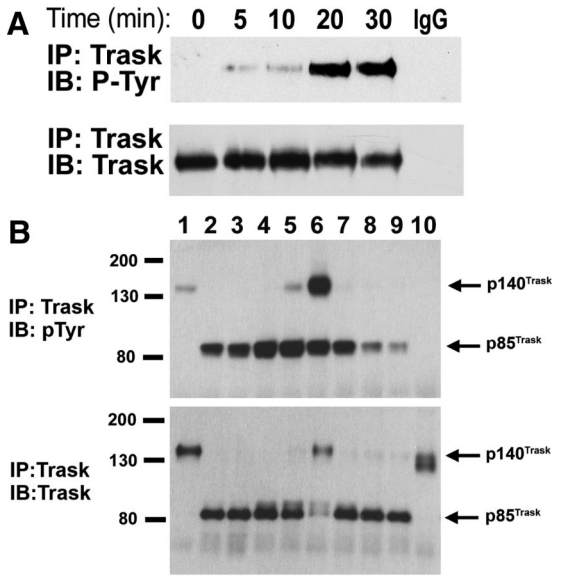

Figure 3. Phosphorylation of Trask during experimental cell detachment. **A:** MCF10A cells were placed in a solution containing EDTA and lysates harvested at the indicated time points. The expression and phosphorylation of Trask was determined by the indicated immunoprecipitation and immunoblotting assays. The IgG immunoprecipitation control was done using lysates from the 30-minute time point. **B:** MCF10A cells were induced to detach by treatment with trypsin for 10 minutes and subsequently cultured continuously in the suspended state for up to 24 hours or alternatively allowed to respread on tissue culture treated plates after 2 hours of culture in suspension. The lanes correspond to adherent untreated cells (lane 1), trypsin treated cells after 1 minute (lane 2, some rounded cells), 5 minutes (lane 3, mostly rounded cells), and 8 minutes (lane 4, entirely rounded cells). The rounded and detached cells were kept in suspension for 2 hours (lane 5) or 24 hours (lane 6) in ULC plates. Some cells were returned to tissue culture treated plates after 2 hours of culture in suspension and cultured for an additional 1 hour (lane 7, still mostly round), 1.5 hours (lane 8, mixed round and spread), or 2 hours (lane 9, mostly spread). Lane 10 shows MCF10A cells that were not exposed to trypsin, but were detached by mechanical scraping and maintained in suspension for 5 minutes. Cell lysates were immunoprecipitated using anti-Trask antibodies and immunoblotted with anti-phosphotyrosine (above) or anti-Trask (below) antibodies. Trask is cleaved by trypsin and is seen predominantly in its 85-kDa cleaved form in cells exposed to trypsin. In cells that are subsequently cultured for 24 hours, continued Trask protein synthesis results in the re-emergence of the 140-kDa uncleaved Trask form.

in a lawn of confluent MCF10A cells. In this wound healing assay, MCF10A cells migrate into the scraped wound and fill the wound in 48 hours. Phosphorylated Trask is evident in migrating cells at the wounded edge, in particular in the leading edge of migrating cells, and in particular at the head of actin filaments (Figure 5), further implicating a role in regulating the actin cytoskeleton. The phosphorylation of Trask in migrating cells is modest compared with the intense phosphorylation seen in detached cells.

To determine the expression and phosphorylation of Trask *in vivo* we conducted an immunohistochemical analysis of archival human tissue sections. Trask is widely expressed in many epithelial tissues (Table 1, Figure 6). The intensity of expression varies and is particularly high in squamous epithelia, but also expressed in many other epithelia. Trask expression is not detectable by immunohistochemical analysis in mesenchymal tissues or central nervous system tissues. Trask is also expressed in a subset of hematopoietic precursors.

Anti-phospho-Trask immunostaining showed no evidence of Trask phosphorylation in most of the cells in these normal tissues. However the *in vivo* stains recapitulate the cell culture evidence that Trask is phosphorylated during mitotic or interphase detachment. Many mitotic cells in fixed tissues show intense phosphorylation of Trask. This is most evident in colonic crypts, which have high mitotic activity (Figure 7A). The mitotic nature of detached and hyperphosphorylated cells in colonic crypts was confirmed by immunostaining with anti-phospho-histone H3 antibodies (Figure 7B). Additional stains were done to confirm that the detached mitotic cells are in fact colon epithelial cells and not extrinsic hematopoietic or neuroendocrine cells. In addition, there is frequent interphase phosphorylation of Trask at the apices of intestinal villi (Figure 7C). Apical cells are commonly shed into the lumen and the apical cells with Trask phosphorylation are likely cells that are about to be shed. Intestinal epithelial cells are continuously generated by mitotic activity within the crypts and exfoliation at the apex. Occasional detached mitotic cells, or detached interphase cells in lung alveoli show phosphorylation of Trask (Figure 7D). These *in vivo* data recapitulate the *in vitro* data from cultured cells.

Discussion

We previously reported the identification of Trask, a novel substrate of src kinases, which is phosphorylated during the mitotic phase in epithelial cells. Here we report that the mitotic phosphorylation of Trask is not associated with the cell cycle checkpoints of mitosis, but rather it is associated with the loss of anchorage that accompanies mitotic division in epithelial cells. As such, Trask phosphorylation is not seen in yet-undetached mitotic cells, and persists beyond mitosis into G1 phase and reverses when cells have reattached to matrix. The phosphorylation of Trask is seen in most circumstances of anchorage-deprived epithelial cells including cells experimentally forced into suspension through treatment with EDTA or trypsin, and cancer cell subpopulations or subtypes that spontaneously grow in suspension. More modest phosphorylation of Trask is also seen in the leading edge of migrating epithelial cells. The leading edge of migrating cells are areas of active actin remodeling and it is possible that Trask phosphorylation is involved in the regulation of actin assembly or engagement of the growing actin filaments to the cell membrane or specific membrane microdomains. Indeed, Trask was identified as one of many proteins in a proteomic analysis of the tetraspanin web and it may function to regulate membrane-cytoskeletal interactions within the tetraspanin microdomain.[12] A function of Trask in regulating the actin cytoskeleton is also suggested by overexpression studies wherein the inducible induction of Trask overexpression and overphosphorylation prevents cell spreading and attachment to matrix.[9]

We studied the expression and phosphorylation of Trask in human tissues and find that it is widely expressed in many epithelial tissues including tissues of the

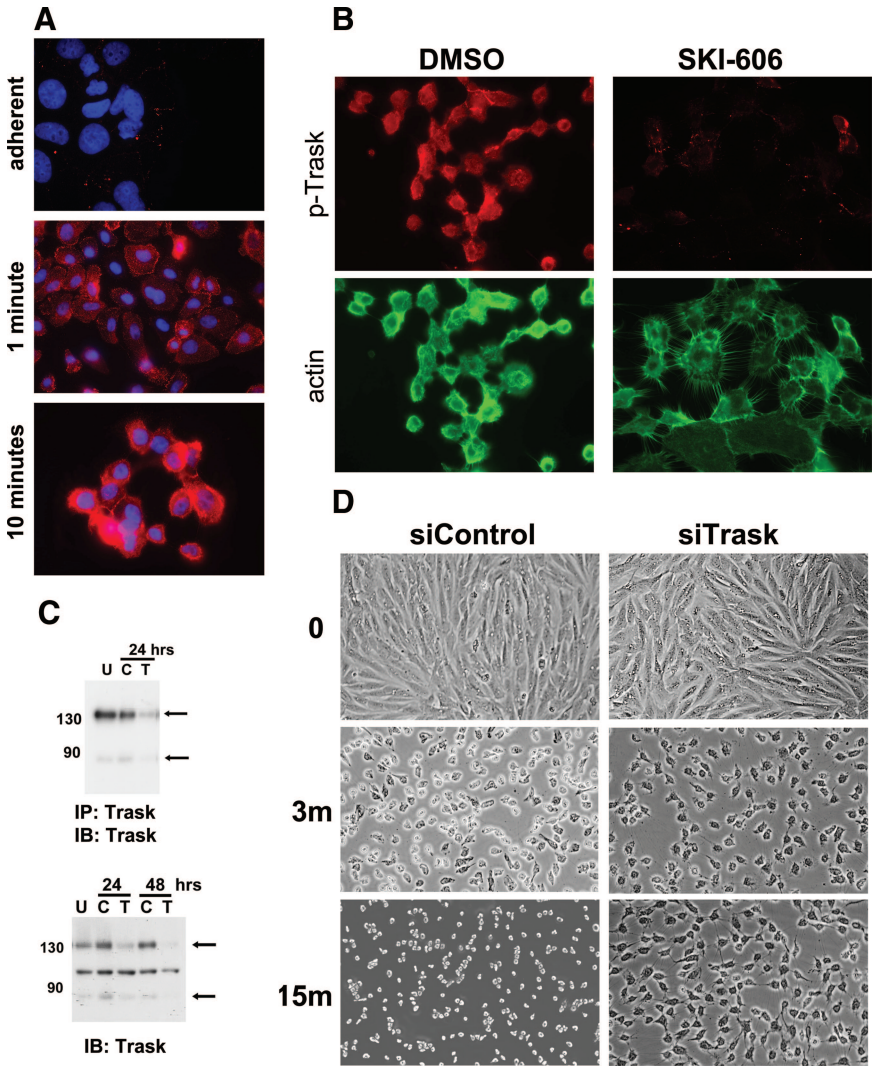

Figure 4. Trask phosphorylation in retracting cells. **A:** MCF10A cells growing on coverslips were placed in a warm solution of trypsin and fixed before or at 1 and 10 minutes into trypsin exposure. Cells were stained with anti-p-Trask antibodies using rhodamine-conjugated secondary reagents. (×1000 magnification) **B:** MCF10A cells were pretreated with 1 μmol/L of the src inhibitor SKI-606 or DMSO for 1 hour to dephosphorylate Trask, and subsequently placed in trypsin for 10 minutes, fixed, and immunostained with anti-p-Trask antibodies and rhodamine-conjugated secondary reagents as well as fluorescein isothiocyanate-conjugated phalloidin to visualize the actin cytoskeleton. (×400 magnification) **C:** MCF10A cells were left untransfected (U) or transfected with anti-Trask siRNA pools (T) or control non-targeting siRNA pools (C). Trask knockdown was verified by anti-Trask immunoblotting (**bottom**). The middle band in these western blots is non-specific background as determined by immunoblot analysis of anti-Trask immunoprecipitates (**top**). **D:** MCF10A cells were transfected with anti-Trask siRNA pools or control non-targeting siRNA pools in different wells of a 12-well cluster. Forty-eight hours later, cells were simultaneously washed and placed in pre-warmed trypsin solution and observed and serially photographed under phase contrast microscopy at the indicated time points (×200 magnification).

respiratory and gastrointestinal tracts, some reproductive and urinary organs, and the skin. There is undetectable expression of Trask in tissues of mesenchymal origin and the central nervous system in these immunohistochemical studies. The fact that Trask is predominantly an epithelial protein and that it is phosphorylated during detachment of epithelial cells suggests that it may be involved in aspects of cell detachment that are uniquely relevant to epithelial cells. Epithelial cells, unlike mesenchymal cells, are abundant in cell–cell junctions including tight junctions, adherens junctions, and gap junctions. These structures provide tissue level structure and

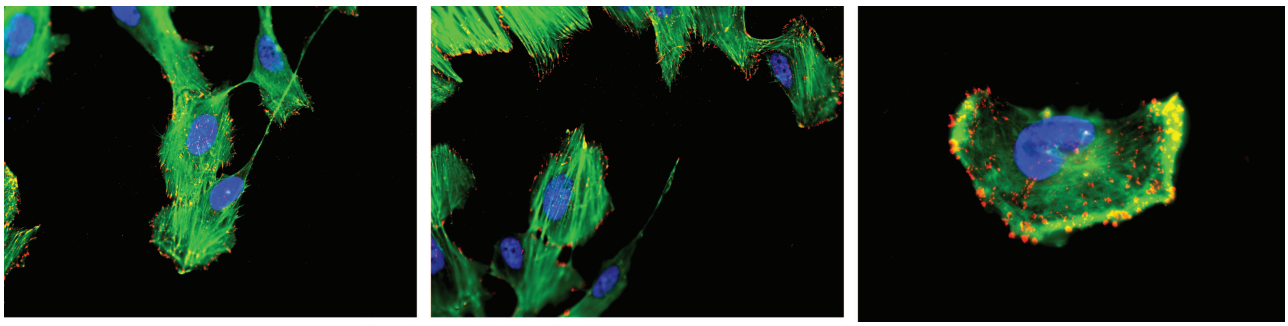

Figure 5. Trask phosphorylation during cell migration. Near-confluent MCF10A cells growing on fibronectin-treated round coverslips were linearly scraped across the equator creating a linear gap within the lawn of cells and placed back in the incubator. These cells typically migrate into the artificially created gap within the following 24 hours of culture. After 8 hours of culture, the cells were fixed and immunostained using anti-phospho-Trask antibodies, rhodamine-conjugated secondary reagents, and fluorescein isothiocyanate-conjugated phalloidin to visualize the actin cytoskeleton. Cells at the migrating edge (**left** 2 images) and within the gap (**right** image) are shown here. (×1000 magnification).

Table 1. Trask Expression in Human Tissues

	Trask	p-Trask
Bladder	3+	0
Kidney	0	0
Tongue	3+	0
Esophagus	3+	0
Stomach	1+	0
Ileum/jejunum	1/2+	0
Colon	2+	0*
Rectum	2+	0
Liver	2+ ducts	0
Pancreas	2+	0
Skin	3+	0
Nevus	0	0
Breast	2+ ducts/lobules	0
Thyroid	0	0
Lung	2+ bronchioles/0 alveoli	0
Testis	0	0
Prostate	1+	0
Cervix	3+	0
Brain	0	0
Cerebellum	0	0
Skeletal muscle	0	0
Myometrium	0	0
Diaphragm	0	0
Heart	0	0
Spleen	0	0
Tonsil	0	0
Thymus	0	0
Adipose	0	0
Bone marrow	2+ primitive myeloid	0

*3+ in apical cells & in detached mitoses.

Sections from the indicated archival tissue sources were prepared and stained with anti-Trask and anti-phospho-Trask antibodies. The staining intensity was scored by two observers according to procedures and definitions described in methods. All immunostains and their analyses were conducted using well defined positive and negative controls as described in Materials and Methods. The scored expression and phosphorylation of Trask is shown for all examined types of tissues.

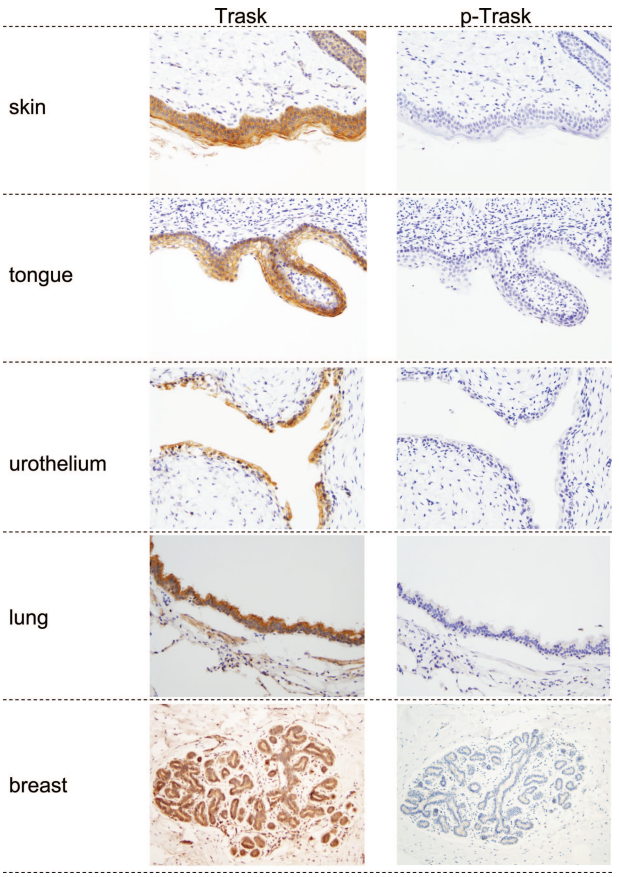

Figure 6. Trask expression and phosphorylation in human tissues. Representative images from immunostaining of selected normal tissues are shown here. Magnifications are ×100 (skin, tongue), ×200 (urothelium), and ×40 (lung, breast).

function attributes to epithelial tissues and they must be reversibly dismantled and reassembled during epithelial cell detachment. Trask may have functions that are relevant to the regulation or assembly of these structures. The expression of Trask we see in some primitive myeloid cells is consistent with a previous report showing that Trask/CDCP1 is expressed in hematopoietic stem cells.[13] Although the expression of Trask/CDCP1 has been characterized in hematopoietic cells, the role of its phosphorylation in the context of this cell type has not been reported. Modulation of the actin cytoskeleton during cell migration, and attachment to endothelium or bone marrow stromal elements are aspects of hematopoietic cells that may be regulated by Trask/CDCP1 phosphorylation.

Our experimental data are not an artifact of *in vitro* cell culture models and are nicely recapitulated by *in vivo* evidence similarly showing the phosphorylation of Trask during mitotic detachment of epithelial cells in the mitotically active colon crypts or rare mitoses in lung alveoli, and during cell detachment, migration, and physiological shedding, such as is seen in the apices of colonic villi. Trask may function to regulate membrane shape and rigidity in detached epithelial cells, or to regulate the adhesion-independent formation of cortical actin in rounded cells, or to mediate anti-proliferative or pro-survival cell signals in detached epithelial cells. Indeed, src kinase activity increases with epithelial cell detachment and this increase has been linked with averting anoikis in detached cells.[14–16] Trask may be the src substrate that mediates this effect as suggested by experiments showing that Trask/CDCP1 knockdown induces anoikis in lung cancer cells.[17] The function of Trask in epithelial tissues will ultimately be defined by genetic mouse models.

Trask is a transmembrane protein and in many cells its membrane expression is clearly evident by immunofluorescence or immunohistochemical microscopy. But in detached and rounded cells with abundant Trask phosphorylation, the membrane localization of p-Trask is less evident. This was noticed in our previous study[9] and in intensely phosphorylated cells in this study (Figures 1A, 3B, 6). Much of this is due to the extreme intensity of the signal during mitosis or detachment. These studies were done using antibody dilutions that were designed to detect slight or modest phosphorylation of Trask, such as those seen in shedding cells (Figure 7C) or in some cancers (data not shown). Therefore much of the cytoplasmic signal seen in intensely phosphorylated cells is likely due to overstaining artifact. In some sections with less intense staining, the p-Trask signal in mitotic cells is more clearly membrane localized (Figure 7B).

A function for Trask/CDCP1 in epithelial tumorigenesis has been suggested by us and others, but the nature of

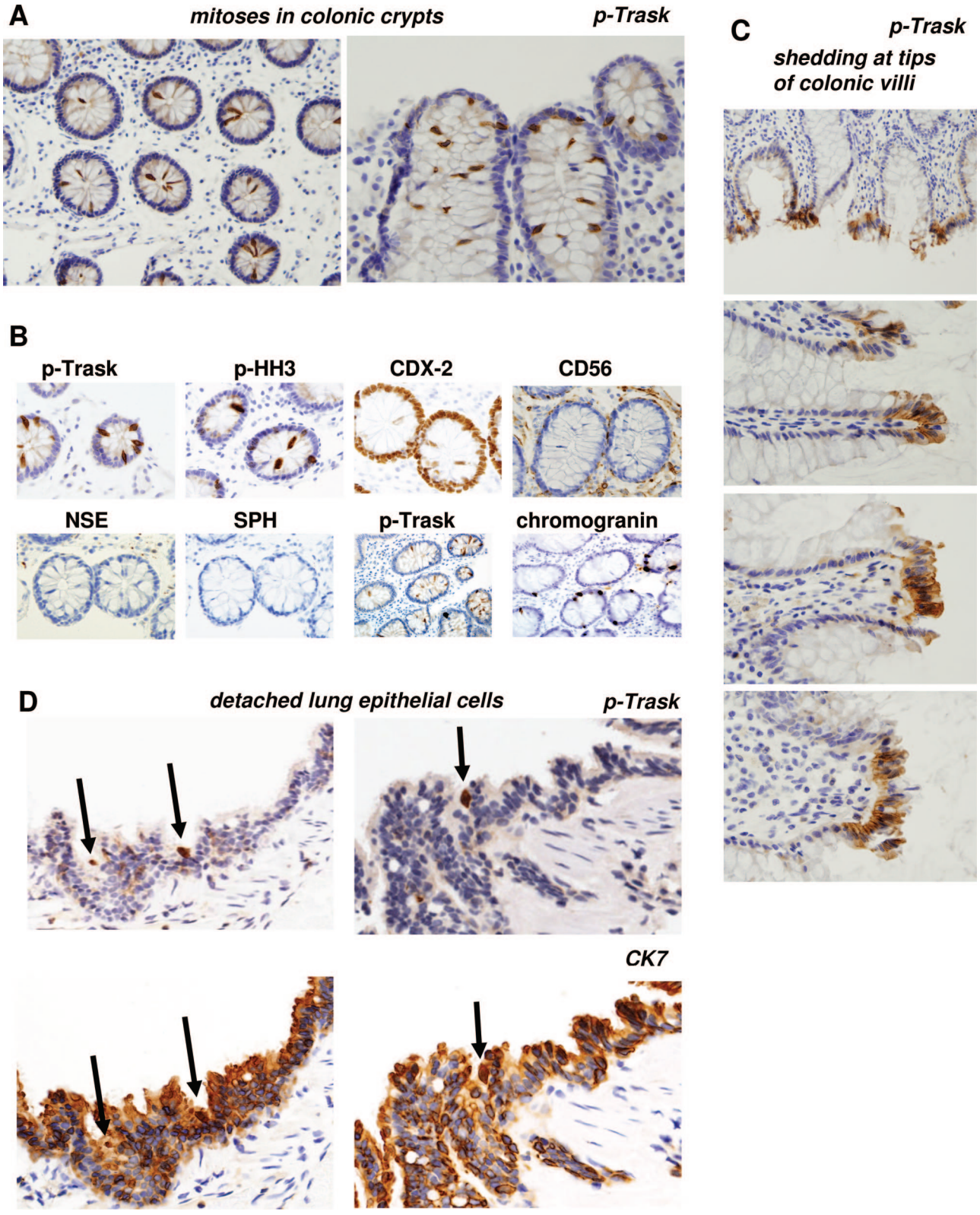

Figure 7. Trask phosphorylation in specific epithelial cells. **A:** Trask phosphorylation is seen in occasional mitotic cells. This is shown here in the mitotically active crypt regions of normal colonic mucosa. ×200 (**left**) and ×400 (**right**) magnifications. **B:** The detaching cells in the crypts were confirmed to be epithelial cells as shown by staining with the intestinal epithelial differentiation marker CDX2, confirmed to be mitotic cells by the mitotic marker phospho-histone H3, and confirmed not to be extrinsic hematopoietic or neuroendocrine cells as shown by the markers CD56, neuron-specific enolase, and synaptophysin. An additional section from an area of the colon rich in neuroendocrine cells identified by chromogranin staining shows that they are distinct from the luminally detached p-Trask positive cells (×400 magnifications). **C:** Trask phosphorylation is also seen in some clusters of cells at the apices of colonic villi where shedding commonly occurs. Magnifications are ×100 (**top**) and ×400 (others). **D:** Trask phosphorylation is seen in isolated detached epithelial cells (**arrows**) in pulmonary alveoli. (×400 magnification).

this function remains to be defined. Some cancer cells such as MDA-468 cells and DU4475 cells used in this study have Trask phosphorylation during interphase, an attribute not seen in the untransformed MCF10A cells or in normal epithelial tissues. Two studies have shown increased Trask/CDCP1 expression in colon carcinomas compared with normal colon tissues.[10,18] An experimental study in a gastric carcinoma model showed that Trask/CDCP1 overexpression increased and siRNA knockdown reduced the migratory characteristics of this cancer cell model.[19] In a subtractive immunization approach to identify cell surface antigens preferentially overexpressed in more highly metastatic variants of Hep3 carcinoma cells, Hooper et al identified Trask/CDCP1 as a surface protein with increased expression in the more metastatic cells.[11] However, in this same study, a survey of cancer cell lines showed no correlation between the expression of Trask/CDCP1 and metastatic activities. Siva et al developed a toxin-conjugated anti-Trask/CDCP1 antibody that showed cell killing activity *in vitro* and anti-tumor activity *in vivo*.[20] Although interesting, the off target effects of an anti-Trask/CDCP1 immunotoxin approach are underestimated by a mouse model unless the immunotoxin equally targets the mouse antigen. In our study, we find widespread expression of Trask in many human epithelial tissues, including intense expression in some tissues, raising concerns about immunotoxin therapy approaches.

Trask is a recently identified epithelial transmembrane protein widely expressed in many epithelial tissues. Preliminary evidence suggests a function in cell adhesion, cell migration, or cytoskeletal regulation. Further studies are required to further define the functions of Trask in epithelial tissues during development, wound repair, and tumorigenesis and the intracellular and extracellular signaling partners that mediate its functions.

Acknowledgments

We acknowledge the services of the Immunohistochemical and Tissue Cores of the University of California San Francisco Comprehensive Cancer Center in this work, and in particular the technical assistance of Lorretta Chan of the immunohistochemical core.

References

1. Lee JM, Dedhar S, Kalluri R, Thompson EW: The epithelial-mesenchymal transition: new insights in signaling, development, and disease. J Cell Biol 2006, 172:973–981
2. Courtneidge SA, Fumagalli S: A mitotic function for Src? Trends in Cell Biol 1994, 4:345–347
3. Taylor SJ, Shalloway D: Src and the control of cell division. [Review] [40 refs]. Bioessays 1996, 18:9–11
4. Chackalaparampil I, Shalloway D: Altered phosphorylation and activation of pp60c-src during fibroblast mitosis. Cell 1988, 52:801–810
5. Park J, Cartwright CA: Src activity increases and Yes activity decreases during mitosis of human colon carcinoma cells. Mol Cell Biol 1995, 15:2374–2382
6. Morgan DO, Kaplan JM, Bishop JM, Varmus HE: Mitosis-specific phosphorylation of p60 c-src by p34 cdc2-associated protein kinase. Cell 1989, 57:775–786
7. David-Pfeuty T, Nouvian-Dooghe Y: Immunolocalization of the cellular src protein in interphase and mitotic NIH c-src overexpresser cells. J Cell Biol 1990, 111:3097–3116
8. Bagrodia S, laudano AP, Shalloway D: Accessibility of the c-src SH2 domain for binding is increased during mitosis. J Biol Chem 1994, 269:10247–10251
9. Bhatt AS, Erdjument-Bromage H, Tempst P, Craik CS, Moasser MM: Adhesion signaling by a novel mitotic substrate of src kinases. Oncogene 2005, 24:5333–5343
10. Scherl-Mostageer M, Sommergruber W, Abseher R, Hauptmann R, Ambros P, Schweifer N: Identification of a novel gene. CDCP1, overexpressed in human colorectal cancer. Oncogene 2001, 20:4402–4408
11. Hooper JD, Zijlstra A, Aimes RT, Liang H, Claassen GF, Tarin D, Testa JE, Quigley JP: Subtractive immunization using highly metastatic human tumor cells identifies SIMA135/CDCP1, a 135 kDa cell surface phosphorylated glycoprotein antigen. Oncogene 2003, 22:1783–1794
12. Andre M, Le Caer JP, Greco C, Planchon S, El Nemer W, Boucheix C, Rubinstein E, Chamot-Rooke J, Le Naour F: Proteomic analysis of the tetraspanin web using LC-ESI-MS/MS and MALDI-FTICR-MS. Proteomics 2006, 6:1437–1449
13. Conze T, Lammers R, Kuci S, Scherl-Mostageer M, Schweifer N, Kanz L, Buhring HJ: CDCP1 is a novel marker for hematopoietic stem cells. Ann NY Acad Sci 2003, 996:222–226
14. Wei L, Yang Y, Zhang X, Yu Q: Altered regulation of Src upon cell detachment protects human lung adenocarcinoma cells from anoikis. Oncogene 2004, 23:9052–9061
15. Loza-Coll MA, Perera S, Shi W, Filmus J: A transient increase in the activity of Src-family kinases induced by cell detachment delays anoikis of intestinal epithelial cells. Oncogene 2005, 24:1727–1737
16. Windham TC, Parikh NU, Siwak DR, Summy JM, McConkey DJ, Kraker AJ, Gallick GE: Src activation regulates anoikis in human colon tumor cell lines. Oncogene 2002, 21:7797–7807
17. Uekita T, Jia L, Narisawa-Saito M, Yokota J, Kiyono T, Sakai R: CUB domain-containing protein 1 is a novel regulator of anoikis resistance in lung adenocarcinoma. Mol Cell Biol 2007, 27:7649–7660
18. Perry SE, Robinson P, Melcher A, Quirke P, Buhring HJ, Cook GP, Blair GE: Expression of the CUB domain containing protein 1 (CDCP1) gene in colorectal tumour cells. FEBS Lett 2007, 581:1137–1142
19. Uekita T, Tanaka M, Takigahira M, Miyazawa Y, Nakanishi Y, Kanai Y, Yanagihara K, Sakai R: CUB-domain-containing protein 1 regulates peritoneal dissemination of gastric scirrhous carcinoma. Am J Pathol 2008, 172:1729–1739
20. Siva AC, Wild MA, Kirkland RE, Nolan MJ, Lin B, Maruyama T, Yantiri-Wernimont F, Frederickson S, Bowdish KS, Xin H: Targeting CUB domain-containing protein 1 with a monoclonal antibody inhibits metastasis in a prostate cancer model. Cancer Res 2008, 68:3759–3766